Published in Journal of Cluster Science 21, issue 3, 313-324, 2010
which should be used for any reference to this work

Synthesis and Anticancer Activity of Long-Chain Isonicotinic Ester Ligand-Containing Arene Ruthenium Complexes and Nanoparticles

Georg Süss-Fink · Farooq-Ahmad Khan · Lucienne Juillerat-Jeanneret · Paul J. Dyson · Anna K. Renfrew

Abstract Arene ruthenium complexes containing long-chain *N*-ligands $L^1 = NC_5H_4$–4-COO–C_6H_4–4-O–$(CH_2)_9$–CH_3 or $L^2 = NC_5H_4$–4-COO–$(CH_2)_{10}$–O–C_6H_4–4-COO–C_6H_4–4-C_6H_4–4-CN derived from isonicotinic acid, of the type [(arene)Ru(L)Cl_2] (arene = C_6H_6, L = L^1: **1**; arene = *p*-$MeC_6H_4Pr^i$, L = L^1: **2**; arene = C_6Me_6, L = L^1: **3**; arene = C_6H_6, L = L^2: **4**; arene = *p*-$MeC_6H_4Pr^i$, L = L^2: **5**; arene = C_6Me_6, L = L^2: **6**) have been synthesized from the corresponding [(arene)$RuCl_2]_2$ precursor with the long-chain *N*-ligand L in dichloromethane. Ruthenium nanoparticles stabilized by L^1 have been prepared by the solvent-free reduction of **1** with hydrogen or by reducing [(arene)Ru$(H_2O)_3]SO_4$ in ethanol in the presence of L^1 with hydrogen. These complexes and nanoparticles show a high anticancer activity towards human ovarian cell lines, the highest cytotoxicity being obtained for complex **2** (IC_{50} = 2 μM for A2780 and 7 μM for A2780cisR).

Keywords Ruthenium nanoparticles · Anticancer drugs · Bioorganometallic chemistry · Isonicotinic ester ligands · Arene ruthenium complexes

This article is dedicated to Professor Malcolm Chisholm on the occasion of his 65th birthday.

G. Süss-Fink (✉) · F.-A. Khan
Institut de Chimie, Université de Neuchâtel, 2009 Neuchâtel, Switzerland
e-mail: georg.suess-fink@unine.ch

L. Juillerat-Jeanneret
University Institute of Pathology, Centre Hospitalier Universitaire Vaudois (CHUV),
1011 Lausanne, Switzerland

P. J. Dyson · A. K. Renfrew
Institut des Sciences et Ingénierie Chimiques, Ecole Polytechnique Fédérale de Lausanne (EPFL),
1015 Lausanne, Switzerland

Introduction

Arene ruthenium complexes containing chloro ligands are both lipophilic and water-soluble, which preconditions these organometallics for bio-medical applications such as anticancer agents [1]. The field of antitumoural and antimetastatic arene ruthenium complexes has, in recently years, received considerable attention [2, 3], following the notion of using arene ruthenium compounds as anticancer agents by Tocher et al. in 1992, who observed a cytotoxicity enhancement by coordinating the anticancer agent metronidazole [1-β-(hydroxyethyl)-2-methyl-5-nitro-imidazole] to a benzene ruthenium dichloro fragment [4]. The prototype arene ruthenium(II) complexes evaluated for anticancer properties in 2001 were (p-$MeC_6H_4Pr^i$)Ru(P-pta)Cl_2 (pta = 1,3, 5-triaza-7-phospha-tricyclo-[3.3.1.1]decane), termed RAPTA-C [5], and [(C_6H_5Ph)-Ru(N,N-en)Cl][PF_6] (en = 1,2-ethylenediamine) [6].

Isonicotinic acid is widely used for the synthesis of antibiotics and antituberculosis preparations [7], and it has strong bactericide effects [8]. We have been interested in the use of long-chain isonicotinic esters as lipophilic components in order to increase the anticancer activity of arene ruthenium complexes, while at the same time, using a molecule that is known to be tolerated in vivo. Only one arene ruthenium complex containing isonicotinic acid has been reported so far, namely [(C_6H_6)Ru(NC_5H_4COOH)] by Małecki et al. [9], but the biological properties of the complex were not studied.

In this paper we describe the synthesis and characterization of arene ruthenium complexes of the type [(arene)Ru(L)Cl_2] containing long-chain isonicotinic ester ligands L and of ruthenium nanoparticles stabilized by these ligands, and in addition, the cytotoxicity of these agents is reported.

Experimental Section

Synthesis

Solvents were dried using appropriate drying agents and distilled prior to use. $RuCl_3 \cdot 3\ H_2O$ (Johnson-Matthey), 1-bromodecane (Sigma-Aldrich), isonicotinoyl chloride hydrochloride (Sigma-Aldrich), hydroquinone (Sigma-Aldrich) were used as received. NMR spectra were recorded on a Bruker DRX 400 MHz spectrometer at 400.13 (^{1}H) with $SiMe_4$ as internal references and coupling constants are given in Hz. Infrared spectra were recorded on Perkin-Elmer FT-IR spectrometer as KBr pellets. UV–Vis studies were recorded on a UVIKON 930 spectrometer. For the ruthenium nanoparticles, the particle size was determined using a transmission electron microscope, Philips CM 200 operating at 200 K, and the chemical analysis determined by Energy Dispersive X-ray spectroscopy. The compounds [(C_6H_6)$RuCl_2$]$_2$ [10], [(p-$MeC_6H_4Pr^i$)$RuCl_2$]$_2$ [11], [(C_6Me_6)$RuCl_2$]$_2$ [12], [(C_6H_6)-Ru(H_2O)$_3$]SO_4 [13], [(p-$MeC_6H_4Pr^i$)Ru(H_2O)$_3$]SO_4 [14] and [(C_6Me_6)Ru(H_2O)$_3$]SO_4 [15], 4-(decyloxy)phenyl isonicotinate (L^1) [16] and 4′-cyanobiphenyl-4-yl-4-(10-hydroxydecyloxy)benzoate [17] were prepared according to published methods.

Preparation of the New Ligand L^2

4′-Cyanobiphenyl-4-yl 4-(10-hydroxydecyloxy)benzoate (0.1 g, 0.21 mmol) and triethylamine (0.021 g, 0.21 mmol) were dissolved in CH_2Cl_2 (100 mL) and isonicotinoyl chloride hydrochloride (0.09 g, 0.63 mmol) was added. The reaction mixture was stirred overnight at room temperature. The precipitate formed was filtered off and discarded and the solution was evaporated to dryness. The yellow residue obtained was recrystallized several times from ethanol to give a white product, yield: 0.104 g, 85%. (Found: C, 74.87; H, 6.36; N, 4.76. Calc. for $C_{36}H_{36}N_2O_5$ ($M = 576$): C, 74.98; H, 6.29; N, 4.86%). IR (KBr, cm^{-1}): 2920(m), 2223(w, *v*CN), 1723(s, *v*COO), 1604(s), 1493(m), 1255(s), 1162(s). ^{1}H NMR (400 MHz, $CDCl_3$) δ ppm 8.89 (d, $J = 6.0$ Hz, 2H), 8.17 (d, $J = 8.8$ Hz, 2H), 7.86 (d, $J = 6.0$ Hz, 2H), 7.75 (d, $J = 8.4$ Hz, 2H), 7.70 (d, $J = 8.4$ Hz, 2H), 7.65 (d, $J = 8.8$ Hz, 2H), 7.34 (d, $J = 8.8$ Hz, 2H), 6.99 (d, $J = 9.2$ Hz, 2H), 4.36 (t, $J = 6.8$ Hz, 2H), 4.05 (t, $J = 6.8$ Hz, 2H), 1.81 (m, 4H), 1.54–1.32 (m, 12H). MS (ESI) *m/z*: 599.3 $[M+Na]^+$. UV–Vis (CH_2Cl_2): λ_{max} 278 (220124), 228 (56183) nm.

*Preparation of the Complexes [(arene)Ru(L)Cl$_2$] (**1–6**)*

A mixture of the appropriate $[(arene)RuCl]_2$ dimer (0.15 g) and two equivalents of the ligand L^1 or L^2 in CH_2Cl_2 solution (25 mL) was stirred for 3 h at room temperature. The solvent was then removed under reduced pressure, and the residue was dissolved in EtOH (30 mL). Then the solvent was evaporated to dryness, and the final product was collected and dried in vacuo.

[(C_6H_6)Ru(L^1)Cl$_2$], **1**: yield: 0.363 g, > 99%. (Found: C, 55.03; H, 5.83; N, 2.25. Calc. for $C_{28}H_{35}Cl_2NO_3Ru{\cdot}0.1\ CH_2Cl_2$ ($M = 613.5$): C, 54.96; H, 5.78; N, 2.28%). IR (KBr, cm^{-1}): 2925(m), 1747(m, *v*COO), 1631(m), 1505(m), 1277(w), 1192(m). ^{1}H NMR (400 MHz, CD_2Cl_2) δ ppm 9.31 (d, $J = 6.0$ Hz, 2H), 8.00 (d, $J = 6.0$ Hz, 2H), 7.11 (d, $J = 8.8$ Hz, 2H), 6.92 (d, $J = 8.8$ Hz, 2H), 5.65 (s, 6H), 3.95 (t, $J = 6.6$ Hz, 2H), 1.76 (m, 2H), 1.46–1.26 (m, 14H), 0.86 (t, $J = 6.8$ Hz, 3H). MS (ESI) *m/z*: 452.9 $[(M\text{-}\{C_6H_4O(CH_2)_9CH_3\})+Me_2CO+Na]^+$, 391$[(M\text{-}\{C_6H_4OC_{10}H_{21}\})+H_2O+H]^+$. UV–Vis ($CH_2Cl_2$): λ_{max} 337 (4308), 276 (6671), 230 (21465) nm.

[(p-Me$C_6H_4Pr^i$)Ru(L^1)Cl$_2$], **2**: yield: 0.324 g, >99%. (Found: C, 58.17; H, 6.57; N, 2.06. Calc. for $C_{32}H_{43}Cl_2NO_3Ru$ ($M = 661.17$): C, 58.09; H, 6.55; N, 2.12%). IR (KBr, cm^{-1}): 2925(m), 1745(m, *v*COO), 1631(m), 1505(m), 1250(m), 1187(m). ^{1}H NMR (400 MHz, $CDCl_3$) δ ppm 9.31 (d, $J = 6.8$ Hz, 2H), 7.98 (d, $J = 6.4$ Hz, 2H), 7.11 (d, $J = 9.2$ Hz, 2H), 6.93 (d, $J = 9.2$ Hz, 2H), 5.49 (d, $J = 5.6$ Hz, 2H), 5.26 (d, $J = 6.0$ Hz, 2H), 3.96 (t, $J = 6.6$ Hz, 2H), 3.05–2.98 (m, 1H), 2.13 (s, 3H), 1.82–1.75 (m, 2H), 1.48–1.28 (m, 18H), 0.87 (t, $J = 6.8$ Hz, 3H). MS(ESI) *m/z*: 565.0 $[(M\text{-}\{OC_{10}H_{21}\})+Me_2CO+H]^+$. UV–Vis ($CH_2Cl_2$): λ_{max} 340 (5135), 275 (6882), 230 (21482) nm.

[(C_6Me_6)Ru(L^1)Cl$_2$], **3**: yield: 0.309 g, >99%. (Found: C, 59.02; H, 6.84; N, 1.98. Calc. for $C_{34}H_{47}Cl_2NO_3Ru$ ($M = 689.20$): C, 59.21; H, 6.87; N, 2.03%). IR (KBr, cm^{-1}): 2923(s), 1740(s, *v*COO), 1631(w), 1502(s), 1275(m), 1184(s). ^{1}H NMR (400 MHz, *CDCl$_3$*) δ ppm 9.08 (d, $J = 6.4$ Hz, 2H), 7.96 (d, $J = 6.4$ Hz,

2H), 7.11 (d, $J = 8.8$ Hz, 2H), 6.93 (d, $J = 9.2$ Hz, 2H), 3.96 (t, $J = 6.4$ Hz, 2H), 2.02 (s, 18H), 1.79 (m, 2H), 1.47–1.27 (m, 14H), 0.88 (t, $J = 6.6$ Hz, 3H). MS(ESI) *m/z*: 620.1 $[(M\text{-}2Cl)+H]^+$. UV–Vis (CH_2Cl_2): λ_{max} 354 (5349), 277 (6368), 230 (18000) nm.

[(C_6H_6)Ru(L^2)Cl_2], **4**: yield: 0.495 g, >99%. (Found: C, 60.62; H, 5.10; N, 3.29. Calc. for $C_{42}H_{42}Cl_2N_2O_5Ru{\cdot}0.1\ CH_2Cl_2$ ($M = 834.55$): C, 60.54; H, 5.09; N, 3.35%). IR (KBr, cm^{-1}): 2927(m), 2225(w, *v*CN), 1725(s, *v*COO), 1603(m), 1254(s), 1160(s). 1H NMR (400 MHz, $CDCl_3$) δ ppm 9.28 (d, $J = 6.4$ Hz, 2H), 8.15 (d, $J = 9.2$ Hz, 2H), 7.85 (d, $J = 6.4$ Hz, 2H), 7.74 (d, $J = 8.4$ Hz, 2H), 7.69 (d, $J = 8.4$ Hz, 2H), 7.64 (d, $J = 8.4$ Hz, 2H), 7.33 (d, $J = 8.4$ Hz, 2H), 6.98 (d, $J = 8.8$ Hz, 2H), 5.68 (s, 6H), 4.38 (t, $J = 6.8$ Hz, 2H), 4.06 (t, $J = 6.4$ Hz, 2H), 1.86–1.74 (m, 4H), 1.50–1.34 (m, 12H). MS (ESI): *m/z*: 791.1 $[(M\text{-}Cl)]^+$. UV–Vis (CH_2Cl_2): λ_{max} 278 (71012), 229 (28025) nm.

[(p-$MeC_6H_4Pr^i$)Ru(L^2)Cl_2], **5**: yield: 0.432 g, >99%. (Found: C, 62.51; H, 5.80; N, 3.07. Calc. for $C_{46}H_{50}Cl_2N_2O_5Ru$ ($M = 882.21$): C, 62.58; H, 5.71; N, 3.17%). IR (KBr, cm^{-1}): 2927(m), 2227(w, *v*CN), 1731(s, *v*COO), 1606(m), 1261(s), 1168(s). ^{1}H NMR (400 MHz, *$CDCl_3$*) δ ppm 9.23 (d, $J = 6.4$ Hz, 2H), 8.16 (d, $J = 8.8$ Hz, 2H), 7.84 (d, $J = 6.0$ Hz, 2H), 7.74 (d, $J = 8.0$ Hz, 2H), 7.69 (d, $J = 8.4$ Hz, 2H), 7.64 (d, $J = 8.4$ Hz, 2H), 7.33 (d, $J = 8.8$ Hz, 2H), 6.99 (d, $J = 8.8$ Hz, 2H), 5.45 (d, $J = 6.0$ Hz, 2H), 5.24 (d, $J = 6.0$ Hz, 2H), 4.37 (t, $J = 6.6$ Hz, 2H), 4.06 (t, $J = 6.4$ Hz, 2H), 3.04–2.95 (m, 1H), 2.10 (s, 3H), 1.85–1.76 (m, 4H), 1.49–1.31 (m, 18H). MS (ESI) *m/z*: 650.9 $[(M\text{-}\{OC_6H_4\text{-}COOC_6H_4C_6\ H_4CN\})+Me_2CO+Na+H]^+$. UV–Vis ($CH_2Cl_2$): λ_{max} 334 (4558), 279 (47199), 229 (18313) nm.

[(C_6Me_6)Ru(L^2)Cl_2], 6: yield: 0.408 g, > 99%. (Found: C, 61.30; H, 5.87; N, 2.92. Calc. for $C_{48}H_{54}Cl_2N_2O_5Ru \cdot 0.5\ CH_2Cl_2$ ($M = 952.22$): C, 61.10; H, 5.81; N, 2.94%). IR (KBr, cm^{-1}): 2924(m), 2226(w, *v*CN), 1722(s, *v*COO), 1602(s), 1260(s), 1166(s). ^{1}H NMR (400 MHz, $CDCl_3$) δ ppm 9.01 (d, $J = 6.8$ Hz, 2H), 8.15 (d, $J = 8.8$ Hz, 2H), 7.81 (d, $J = 6.4$ Hz, 2H), 7.74 (d, $J = 8.4$ Hz, 2H), 7.69 (d, $J = 8.4$ Hz, 2H), 7.64 (d, $J = 8.4$ Hz, 2H), 7.33 (d, $J = 8.4$ Hz, 2H), 6.99 (d, $J = 9.2$ Hz, 2H), 4.36 (t, $J = 6.6$ Hz, 2H), 4.05 (t, $J = 6.6$ Hz, 2H), 2.00 (s, 18H), 1.85–1.74 (m, 4H), 1.50–1.34 (m, 12H). MS (ESI) *m/z*: 635.0 $[(M\text{-}\{C_6H_4\ COOC_6H_4C_6H_4CN\})+Na]^+$. UV–Vis ($CH_2Cl_2$): λ_{max} 349 (4318), 278 (46268), 229 (16888) nm.

Preparation of the Ruthenium Nanoparticles (7–10)

The L^1-stabilized Ru nanoparticles **7** were prepared by reducing **1** (5 mg, 8.26×10^{-3} mmol) under solvent-free conditions in a magnetically stirred stainless-steel autoclave (volume 100 mL) with H_2 (50 bar) at 100 °C for 64 h. Alternatively, the L^1-stabilized Ru nanoparticles **8–10** were obtained by reacting 5 mg of $[(arene)Ru(H_2O)_3]SO_4$ (for **8** arene = C_6H_6; for **9** arene = *p*-$MeC_6H_4Pr^i$; for **10** arene = C_6Me_6) with one equivalent of ligand L^1 in absolute ethanol (1 mL) in a magnetically stirred stainless-steel autoclave (volume 100 mL) under 50 bar pressure of H_2 at 100 °C for 14 h. After pressure release, the solvent was removed and the nanoparticles were dried in vacuo. The characterization of the nanoparticles

L \ arene	C_6H_6	*p*-$MeC_6H_4Pr^i$	C_6Me_6
L^1	**1**	**2**	**3**
L^2	**4**	**5**	**6**

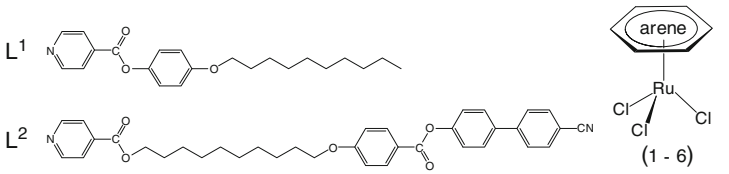

Scheme 1 Synthesis of complexes [(arene)Ru(L)Cl_2] (**1–6**)

7–10 is presented in Figs. 1, 2, 3, and 4. The size distribution of the ruthenium(0) nanoparticles was studied by transmission electron microscopy (TEM) using the "ImageJ" software [18] for image processing and analysis. The mean particle size was estimated from image analysis of ca. 100 particles at least.

Cytotoxicity test (MTT assay)

Cytotoxicity was determined using the MTT assay (MTT=3-(4,5-dimethyl-2-thiazolyl)-2,5-diphenyl-2H-tetrazolium bromide. Cells were seeded in 96-well plates as monolayers with 100 µl of cell solution (approximately 20,000 cells) per well and preincubated for 24 h in medium supplemented with 10% FCS. Compounds were added as DMSO solutions and serially diluted to the appropriate concentration (to give a final DMSO concentration of 0.5%). The concentration of the nanoparticle solutions used in the cytotoxicity assays is based on the concentration of ruthenium in the precursor present in the solution used to prepare the nanoparticles and assuming quantitative conversion. 100 µl of drug solution was added to each well and the plates were incubated for another 72 h. Subsequently, MTT (5 mg/mL solution in phosphate buffered saline) was added to the cells and the plates were incubated for a further 2 h. The culture medium was aspirated, and the purple formazan crystals formed by the mitochondrial dehydrogenase activity of vital cells were dissolved in DMSO. The optical density, directly proportional to the number of surviving cells, was quantified at 540 nm using a multiwell plate reader and the fraction of surviving cells was calculated from the absorbance of untreated control cells. Evaluation is based on means from two independent experiments, each comprising three microcultures per concentration level.

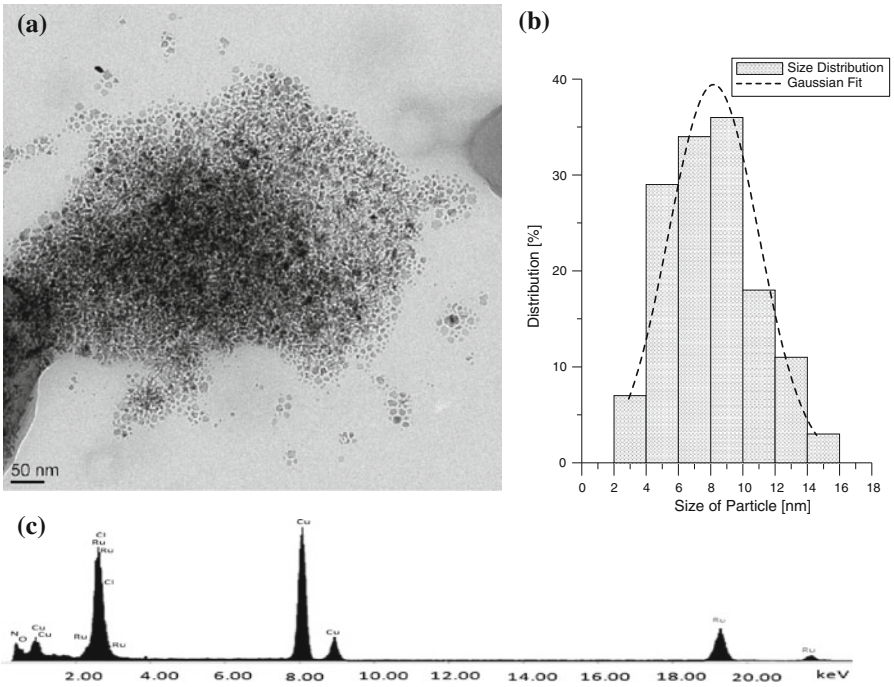

Fig. 1 TEM micrograph (**a**) histogram (**b**) and EDS analysis (**c**) of ruthenium nanoparticles **7**

Results and Discussion

The dinuclear complexes $[(C_6H_6)RuCl_2]_2$, $[(p\text{-}MeC_6H_4Pr^i)RuCl_2]_2$ and $[(C_6Me_6)\text{-}RuCl_2]_2$ react in dichloromethane with two equivalents of the isonicotinic ester L^1 or L^2 to give the neutral complexes [(arene)Ru(L)Cl_2] (**1**–**6**) in quantitative yield, see Scheme 1. All the complexes are obtained as air-stable yellow to yellow/brown powders, which are soluble in polar organic solvents, in particular in dichloromethane and in chloroform. The complexes are also sparingly soluble in water.

$$[(\text{arene})RuCl_2]_2 + L \rightarrow 2[(\text{arene})Ru(L)Cl_2]$$

The solventless reduction of solid $[(C_6H_6)Ru(L^1)]$ (**1**) with H_2 (50 bar, 50 °C) gives ruthenium nanoparticles **7** stabilized by the isonicotinic ester ligand L^1, which have a mean particle size of 8.5 nm (established by TEM). The size distribution of these nanoscopic ruthenium particles (2–16 nm) is relatively large.

Smaller ruthenium nanoparticles stabilized by the isonicotinic ester ligand L^1 were obtained by reducing $[(\text{arene})Ru(H_2O)_3]SO_4$ in ethanol at 100 °C with molecular hydrogen (50 bar) in the presence of L^1 (1 equivalent): The ruthenium nanoparticles **8** obtained from $[(C_6H_6)Ru(H_2O)_3]SO_4$ have a mean particle size of 2.8 nm, the Ru nanoparticles **9** obtained from $[(p\text{-}MeC_6H_4Pr^i)Ru(H_2O)_3]SO_4$ have a mean particle size of 2.3 nm, and the Ru nanoparticles **10** obtained from

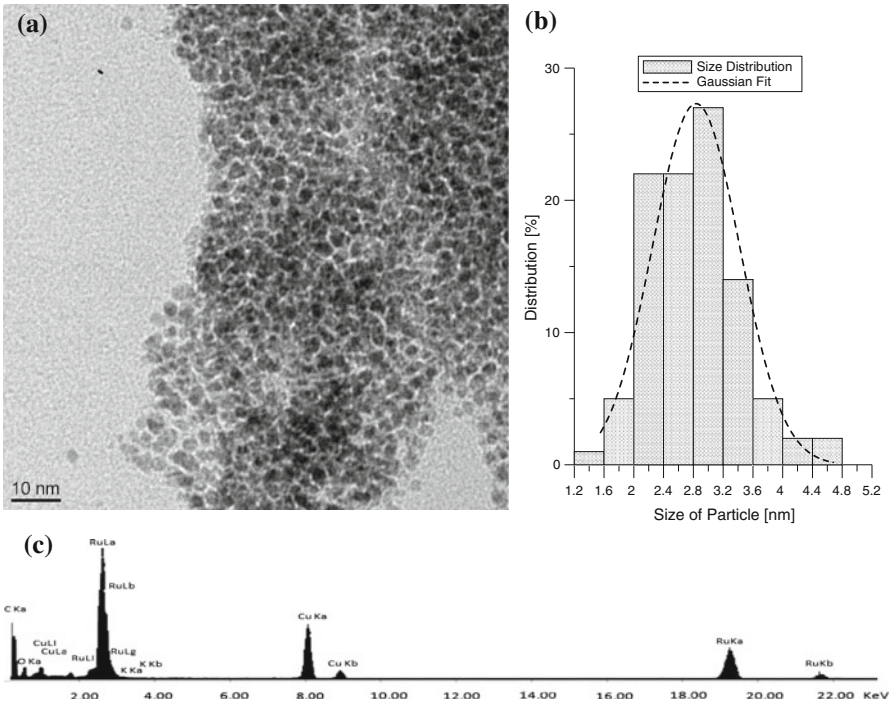

Fig. 2 TEM micrograph (**a**) histogram (**b**) and EDS analysis (**c**) of ruthenium nanoparticles **8**

$[(C_6Me_6)Ru(H_2O)_3]SO_4$ have a mean particle size of 2.2 nm. The ^{1}H NMR spectra of **8–10** in $CDCl_3$ show the presence of the ligand L^1, the signals of the pyridine ring being weak.

The in vitro cytotoxicity of **1–10** has been studied in the A2780 ovarian cancer cell line and cisplatin resistant variant A2780cisR using the MTT assay. Nanoparticles are finding increasing application in medicinal chemistry being used as drug delivery agents, photodynamic therapy, luminescent imaging agents and magnetic imaging agents. In particular, the selective accumulation of nanoparticles in tumour tissue through the enhanced permeability and retention effect, and tunable physical and chemical properties, are attractive properties for such applications [19–22]. The "enhanced permeability and retention" (EPR) effect is a phenomenon in which macromolecules are able to accumulate at the tumour site due to the dramatic increase in blood vessel permeability within diseased tissues compared to normal tissues [23]. To the best of our knowledge, these are the first examples of ruthenium nanoparticles to be evaluated as potential antitumour agents. It should be noted, however, that ruthenium based lipovectors that assemble to form lamellar vesicles have recently been reported [24]. It should be noted that while most attention has been focused towards mononuclear arene ruthenium anticancer compounds [2, 3, 25], there has been increasing interest in polynuclear complexes [26–29], including clusters [30], which display excellent pharmacological properties.

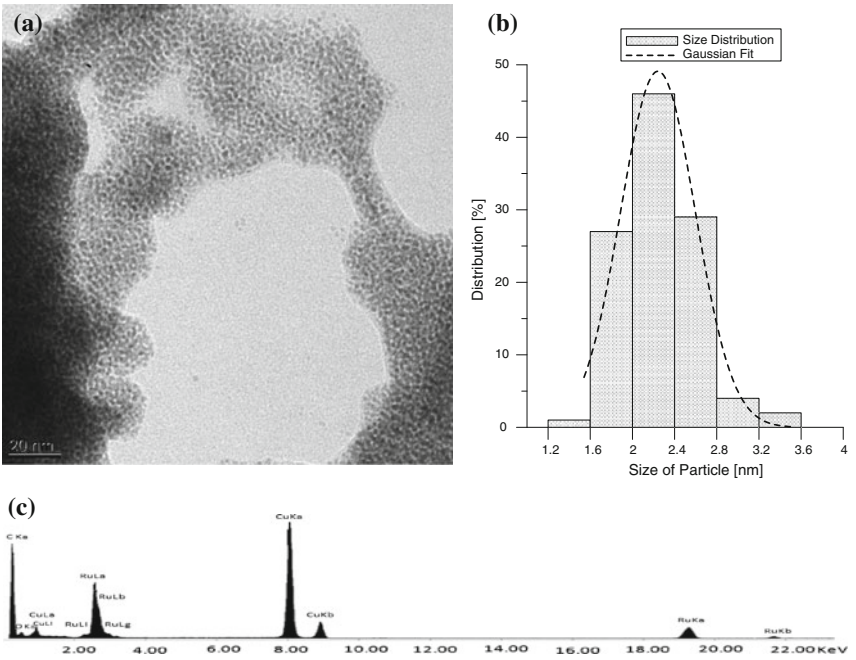

Fig. 3 TEM micrograph (**a**) histogram (**b**) and EDS analysis (**c**) of ruthenium nanoparticles **9**

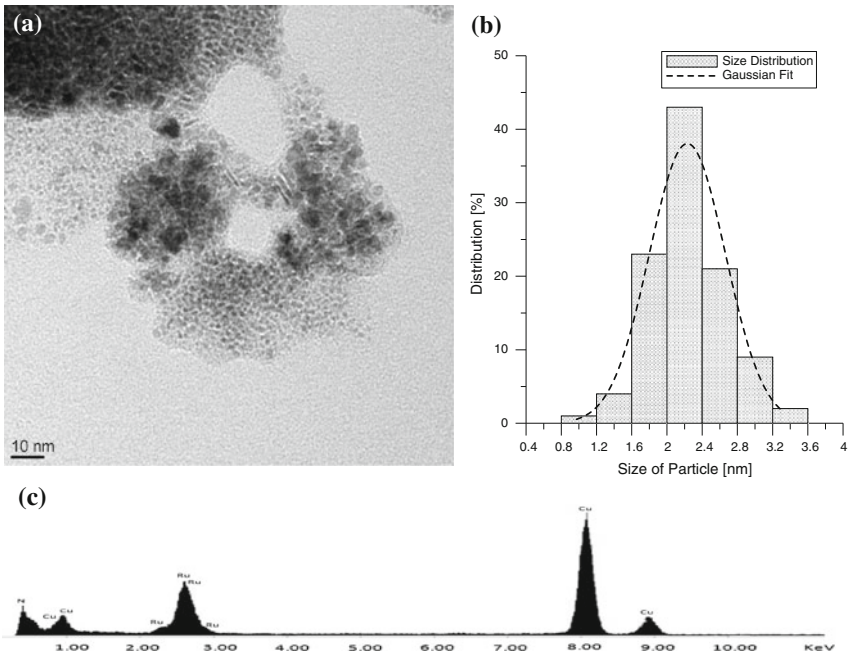

Fig. 4 TEM micrograph (**a**) histogram (**b**) and EDS analysis (**c**) of ruthenium nanoparticles **10**

The monomeric dichloro complexes of ligand L^1 (**1–3**), exhibit very high cytotoxicity in both the A2780 and resistant cell line, see Tables 1 and 2. In particular, the benzene and *p*-cymene complexes have IC_{50} values equivalent to cisplatin in the A2780 line (1.6 μM) and 2–3 fold lower in the cisplatin resistant line A2780cisR [31]. Interestingly, the analogous pyridine complex [(*p*-$MeC_6H_4Pr^i$)-$Ru(py)Cl_2$] is essentially inactive (IC_{50} = 750 μM) under comparable conditions [32], suggesting that the cytotoxicity of **1–3** may be due to the long-chain isonicotinic ester group. This is supported by the very low IC_{50} values observed for the free ligand L^1 (5, 11 μM). In contrast, L^2 exhibited much lower cytotoxicity, as did complexes **4–6**, possibly due to their poorer aqueous solubility.

The L^1-stabilized Ru nanoparticles **7–10**, also exhibit moderate cytotoxicity in the ovarian cancer cell line, with the exception of *p*-cymene derived system **9**, which was unusually inactive (Table 3). For the other compounds, the size of the nanoparticles and nature of the ligands in the precursor complex appears to have little effect on cytotoxicity, with all three compounds exhibiting similar IC_{50} values (29–39 μM). It seems probable that the isonicotinic ester ligand L^1 is important to the in vitro activity of the complexes given that the free ligand is so cytotoxic. In fact, a number of structurally similar isonicotinic esters with long alkyl chains have previously been reported to show interesting biological activity [33–35].

Table 1 Cytotoxicity of complexes **1–6** towards human ovarian cancer cells

	compound	A2780 IC_{50} [μM]	A2780cisR IC_{50} [μM]
1	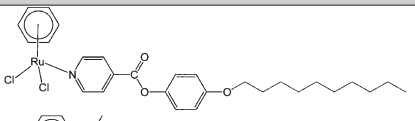	3	10
2	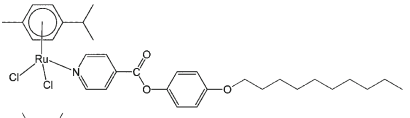	2	7
3	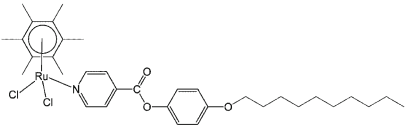	29	28
4	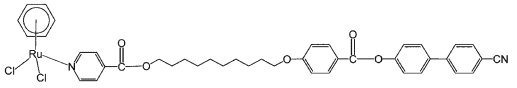	36	264
5	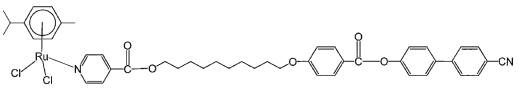	38	253
6	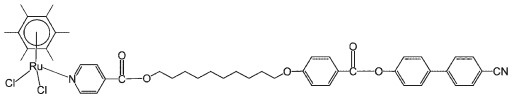	38	278

Table 2 Cytotoxicity of ligands L and arene ruthenium triaqua complexes towards human ovarian cancer cells

	Compound	A2780 IC_{50} [μM]	A2780cisR IC_{50} [μM]
L^1	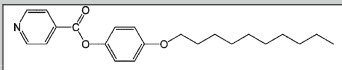	5	11
L^2	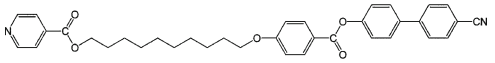	225	303
	$[(C_6H_6)Ru(H_2O)_3]SO_4$	>200	-
	$[(p\text{-}MeC_6H_4Pr^i)Ru(H_2O)_3]\ SO_4$	>200	-
	$[(C_6Me_6)Ru(H_2O)_3]\ SO_4$	74	-

Table 3 Cytotoxicity of nanoparticles **7**–**10** towards human ovarian cancer cells

	Ru nanoparticles	mean size [nm]	A2780 IC_{50} [μM]
7	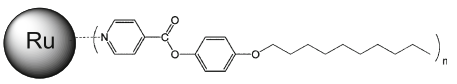	8.5	29
8	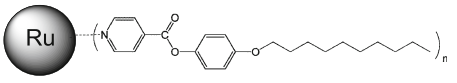	2.8	34
9	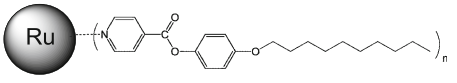	2.3	>200
10	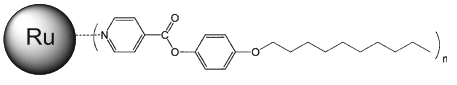	2.2	39

Conclusions

A series of arene ruthenium complexes containing a long-chain *N*-ligands were prepared as were a series of ruthenium-based nanoparticles coated with the same

long-chain ligands. The cytotoxicity of the two series of compounds, i.e. small molecule molecular complexes and nanoparticles, were evaluated in human ovarian cancer cells (A2780). It was found that the small molecules were more cytotoxic than the nanoparticles and while it is difficult to give a reason for this difference it could be due to more efficient uptake of the mononuclear complexes. It is worth noting that for the complexes, the cytotoxicities reflect, to some extent, that of the free ligands. The cytotoxicity of the mononuclear complexes was also established in the cisplatin resistant variant cell line, A2780cisR, and essentially the same degree of resistance was observed for these compounds compared to that of cisplatin. Overall, the similarity in cytotoxicites in the two studied cell lines between **1** and **2** and cisplatin is remarkable, especially for such structurally different compounds. However, it is too early to say whether these ruthenium compounds exert their cytotoxic effect via a similar mechanism to cisplatin or whether different mechanisms are in operation. While the ruthenium nanoparticles are less cytotoxic than the complexes, the fact that they can potentially target tumour tissue selectively via the enhanced permeability and retention effect, still endows them with promise, but an in vivo study is needed to establish whether such systems really can accumulate selectively in tumours.

Acknowledgments Financial support of this work from the Fonds National Suisse de la Recherche Scientifique (Grant no. 200021-115821) is gratefully acknowledged. We also thank the Johnson Matthey Research Centre for a generous loan of ruthenium(III) chloride hydrate.

References

1. G. Süss-Fink (2010). *Dalton Trans.* **39**, 1673.
2. P. J. Dyson (2007). *Chimia.* **61**, 698.
3. S. J. Dougan and P. J. Sadler (2007). *Chimia.* **61**, 704.
4. L. D. Dale, J. H. Tocher, T. M. Dyson, D. I. Edwards, and D. A. Tocher (1992). *Anti-Cancer Drug Design.* **7**, 3.
5. C. S. Allardyce, P. J. Dyson, D. J. Ellis, and S. L. Heath (2001). *Chem. Commun.* 1396.
6. R. E. Morris, R. E. Aird, P. d. S. Murdoch, H. Chen, J. Cummings, N. D. Hughes, S. Pearsons, A. Parkin, G. Boyd, D. I. Jodrell, and P. J. Sadler (2001). *J. Med. Chem.* **44**, 3616.
7. G. V. Tsarichenko, V. I. Bobrov, and M. V. Smarkov (1977). *Pharm. Chem. J.* **11**, 481.
8. J. Suarez, K. Ranguelova, and A. A. Jarzecki (2009). *J. Biol. Chem.* **284**, 7017.
9. J. G. Małecki, R. Kruszynski, M. Jaworska, P. Lodowski, and Z. Mazurak (2008). *J. Organomet. Chem.* **693**, 1096.
10. T. Arthur and T. A. Stephenson (1981). *J. Organomet. Chem.* **208**, 369.
11. M. A. Bennett, G. B. Robertson, and A. K. Smith (1972). *J. Organomet. Chem.* **43**, C41.
12. M. A. Bennett, T. W. Matheson, G. B. Robertson, A. K. Smith, and P. A. Tucker (1980). *Inorg. Chem.* **10**, 1014.
13. M. S. Röthlisberger, W. Hummel, P.-A. Pittet, H.-B. Bürgi, A. Ludi, and A. E. Merbach (1988). *Inorg. Chem.* **27**, 1358.
14. W. Weber and P. C. Ford (1986). *Inorg. Chem.* **25**, 1088.
15. S. Ogo, T. Abura, and Y. Watanabe (2002). *Organometallics.* **21**, 2964.
16. M. Marcos, M. B. Ros, J. L. Serrano, M. A. Esteruelas, E. Sola, L. A. Oro, and J. Barberà (1990). *Chem. Mater.* **2**, 748.
17. B. Dardel, D. Guillon, B. Heinrich, and R. Deschenaux (2001). *J. Mater. Chem.* **11**, 2814.
18. M. D. Abramoff, P. J. Magelhaes, and S. J. Ram (2004). *Biophotonics Int.* **11**, 36.
19. Y. Malam, M. Loizidou, and A. M. Seifalian (2009). *Trends Pharm. Sci.* **30**, 592.

20. P. P. Jumade, A. M. Gupta, P. W. Dhore, P. S. Wake, V. V. Pande, and A. Deshmukh (2009). *J. Chem. Pharm. Sci.* **2**, 158.
21. M. E. Gindy and R. K. Prud'homme (2009). *Exp. Opin. Drug Deliv.* **6**, 865.
22. W. Lin, T. Hyeon, G. M. Lanza, M. Zhang, and T. J. Meade (2009). *MRS Bull.* **34**, 441.
23. D. F. Baban and L. W. Seymour (1998). *Adv. Drug Deliv. Rev.* **34**, 109.
24. M. Vaccaro, R. Del Litto, G. Mangiapia, A. M. Carnerup, G. D'Errico, F. Ruffoa, and L. Paduano (2009). *Chem. Commun.* 1404.
25. W. H. Ang and P. J. Dyson (2006). *Eur. J. Inorg. Chem*. 4003.
26. F. Schmitt, P. Govindaswamy, G. Süss-Fink, W. H. Ang, P. J. Dyson, L. Juillerat-Jeanneret, and B. Therrien (2008). *J. Med. Chem.* **51**, 1811.
27. P. Govender, N. C. Antonels, J. Mattsson, A. K. Renfrew, P. J. Dyson, J. R. Moss, B. Therrien, and G. S. Smith (2009). *J. Organomet. Chem.* **694**, 3470.
28. J. Mattsson, P. Govindaswamy, A. K. Renfrew, P. J. Dyson, P. Štěpnička, G. Süss-Fink, and Bruno. Therrien (2009). *Organometallics.* **28**, 4350.
29. M. G. Mendoza-Ferri, C. G. Hartinger, A. A. Nazarov, R. E. Eichinger, M. A. Jakupec, K. Severin, and B. K. Keppler (2009). *Organometallics.* **28**, 6260.
30. B. Therrien, W. H. Ang, F. Chérioux, L. Vieille-Petit, L. Juillerat-Jeanneret, G. Süss-Fink, and P. J. Dyson (2007). *J. Clust. Sci.* **18**, 741.
31. M. Auzias, B. Therrien, G. Süss-Fink, P. Štěpnička, W. H. Ang, and P. J. Dyson (2008). *Inorg. Chem.* **47**, 578.
32. C. A. Vock, C. Scolaro, A. D. Phillips, R. Scopelliti, G. Sava, and P. J. Dyson (2006). *J. Med. Chem.* **49**, 5552.
33. K. Furuta, H. Shirahashi, H. Yamashita, K. Ashibe, and E. Kuwano (2006). *Biosci. Biotechnol. Biochem.* **70**, 746.
34. W. G. Friebe, W. Kampe, M. Linssen, and O. H. Wilhelms (1992). Ger. Offen. DE 4038335 A1 19920604.
35. D. S. Goldfarb (2009) U.S. Patent Appl. Publ. US 2009163545 A1 20090625.